JOURNAL OF EXPERIMENTAL ZOOLOGY (MOL DEV EVOL) 304B:107–118 (2005)

Hox Code in Embryos of Chinese Soft-Shelled Turtle *Pelodiscus sinensis* Correlates With the Evolutionary Innovation in the Turtle

YOSHIE KAWASHIMA OHYA, SHIGEHIRO KURAKU, AND SHIGERU KURATANI*
Laboratory for Evolutionary Morphology, Center for Developmental Biology (CDB), RIKEN, Kobe 650-0047, Japan

ABSTRACT Turtles have the most unusual body plan of the amniotes, with a dorsal shell consisting of modified ribs. Because this morphological change in the ribs can be described as an axial-level specific alteration, the evolution of the turtle carapace should depend on changes in the *Hox* code. To identify turtle-specific changes in developmental patterns, we cloned several *Hox* genes from the Chinese soft-shelled turtle, *Pelodiscus sinensis*, examined their expression patterns during embryogenesis, and compared them with those of chicken and mouse embryos. We detected possibly turtle-specific derived traits in *Hoxc-6* expression, which is restricted to the paraxial part of the embryo; in the expression of *Hoxa-5* and *Hoxb-5*, the transcripts of which were detected only at the cervical level; and in *Hoxc-8* and *Hoxa-7* expression, which is shifted anteriorly relative to that of the other two amniote groups. From the known functions of the *Hox* orthologs in model animals, these *P. sinensis*-specific changes apparently correlate with specializations in the turtle-specific body plan. *J. Exp. Zool. (Mol. Dev. Evol.) 304B:107–118, 2005.*

INTRODUCTION

The skeletal morphology of turtles is unique among amniotes because of the dorsal carapace and ventral plastron, the partial absence of the epaxial muscles, and the location of the limb girdles. Formation of the turtle carapace is based on the vertebrae and the ribs that arise from the ninth to the 18th vertebrae, which grow laterally into the superficial layer of the body. At this axial level, the epaxial muscles are greatly reduced or lost. Unlike the other amniotes, the ventral ribs are not formed in turtles; instead, the dermal plastron covers the ventral body. In association with these changes, the shoulder girdle is found inside the rib cage, unlike the other vertebrate species in which the scapula develops outside the cage (Ruckes,'29; Burke,'89,'91; Lee,'93; Hall,'98, Gilbert et al., 2001). Furthermore, to allow contraction of the neck into the shell, the cervical vertebrae of modern cryptodires have highly specialized articulation between each cervical vertebra (Romer,'56). These features of turtles are mainly the result of changes in specifications of the axial and paraxial skeletal elements at a specific level along the anteroposterior (A–P) axis.

Turtles are also characterized by their abrupt appearance in the fossil record. *Proganochelys* (Jaekel,'16; Gaffney,'90), the most primitive turtle from the late Triassic, already possessed a shell with internalized limb girdles, as seen in modern species. No intermediate stages have been discovered nor is it possible to postulate any intermediate states leading to the turtle pattern (Burke,'91; Rieppel, 2001), although Lee has proposed that pareiasaurs were the closest relatives of turtles (Lee,'93). These facts lead us to conclude that the establishment of the turtle body plan may have proceeded quickly, and that some fundamental changes in the developmental patterning program altered the basic topography of mesoderm derivatives in the ancestor of the chelonians. These types of evolutionary change, which lead to new patterns by overriding ancestral developmental constraints, have been called ''evolutionary novelties'' (Müller and Wagner, '91). In turtle development, the carapace appears to be an

Grant sponsor: Grants-in-Aid to S.K. from the Ministry of Education, Science and Culture of Japan.
*Correspondence to: Shigeru Kuratani, Laboratory for Evolutionary Morphology, Center for Developmental Biology (CDB), RIKEN, 2-2-3 Minatojima-minami, Chuo-ku, Kobe Hyogo 650-0047, Japan. E-mail: saizo@cdb.riken.jp
Received 5 September 2004; Accepted 21 October 2004
Published online 28 December 2004 in Wiley InterScience (www.interscience.wiley.com). DOI: 10.1002/jez.b.21027

evolutionary novelty based on the dorsal shift of the ribs at the thoracic level.

In vertebrates, like most bilaterian species, morphological specification along the A–P axis is established through the spatially organized expression of a common set of genes, the *Hox* genes, at the phylotypic stage of development (Slack et al.,'93; Burke et al.,'95). The collinear distribution of *Hox* gene transcripts reflects positional values in the spinal cord (Tiret et al.,'98), hindbrain (Goddard et al.,'96), branchial arches (Vieille-Grosjean et al.,'97), paraxial mesoderm (Burke et al.,'95; Favier et al.,'96; Fromental-Ramain et al.,'96), and the lateral plate mesoderm (Nowicki and Burke, 2000). Importantly, the above-noted novelty in the turtle body plan is primarily associated with Hox-expressing mesodermal derivatives (Nowicki and Burke, 2003b). A number of mutational analyses of model animals have demonstrated that the *Hox* genes actually play crucial roles in determining the specification of axial morphology, alone or in concert (Condie and Capecchi,'94; Krumlauf,'94; Davis et al.,'95; Horan et al.,'95; Fromental-Ramain et al.,'96; Manley and Capecchi,'97; Chen et al.,'98; Gavalas et al.,'98; Mak,'98; Studer et al.,'98; Suemori and Noguchi, 2000). Comparative analyses of *Hox* gene expression have shown that the *Hox* expression boundaries correspond to morphological identities of the vertebrae commonly recognized in several different species (Kessel,'92; Burke et al.,'95; Gaunt, 2000). To understand the origin of the turtle body plan from the viewpoint of evolutionary developmental biology, it is thus a prerequisite to examine by comparative methods the expression patterns of turtle *Hox* cognates and to identify the candidates for turtle-specific changes in developmental programs.

We report here the *Hox* expression patterns in the Chinese soft-shelled turtle, *Pelodiscus sinensis*, and compare them with those in chicken and mouse embryos. This is intended to distinguish the turtle-specific patterns of gene expression from those of the other amniotes, which could possibly be associated with the origin of the turtle-specific body plan.

MATERIALS AND METHODS

Embryos

Fertilized eggs of *P. sinensis* were purchased from several local farms in Japan. The eggs were incubated at 30°C, and the embryos were staged according to Tokita and Kuratani (2001). Fertilized White Leghorn chicken eggs were also obtained from a local supplier. The eggs were incubated at 38°C, and embryos were staged according to Hamburger and Hamilton ('51). Mouse embryos were recovered at various times of gestation and staged according to Theiler ('89). For in situ hybridization, embryos of *P. sinensis,* chicken, and mouse were fixed with 4% paraformaldehyde in phosphate-buffered saline (Murakami et al., 2001).

Isolation of Hox cDNAs

P. sinensis Hox cDNA fragments were amplified using primers corresponding to conserved regions within the reported sequences of amniote *Hox* genes. For *PsHoxa-5* cDNA (800 bp), primers pshoxb5H (5′-ATGAGCTCTTACTTTGTAAA-3′) and pshocb5-R (5′-GCTCATGCTTTTCAGTTTATTA-3′); for *PsHoxb-5* cDNA (800 bp), primers pshoxb5H (5′-ATGAGCTCTTACTTTGTAAA-3′) and pshocb5-R (5′- GCTCATGCTTTTCAGTTTATTA-3′); for *PsHoxc-6* cDNA (540 bp), primers cc6F2 (5′-TTATCCTGCCATCTAACCAG-3′) and psc6R2 (5′-TCCTGTTCTGGAACCAGATT-3′); for *PsHoxa-7* cDNA (530 bp), primers CXC53 (5′-ATGAGCTCTTCGTATTATGT-3′) and CXC54 (5′-CTGGAACCAGATCTTGATCT-3′); for *PsHoxb-7* cDNA (650 bp), primers psx3 (5′-ATGAGTTCATTG TATTATGC-3′) and psx4 (5′-TCAGTCTTCCTCCTCATCTT-3′); for *PsHoxc-8* cDNA (730 bp), primers CXC5 (5′- ATGAGTTCCTACTTTGTAAA-3′) and CXC6 (5′-TCAGTCCTTGCTTTCTTCTT-3′). Chicken *Hox* cDNAs and mouse *Hoxc-6* cDNA were amplified using specific primers. Amplified cDNA fragments were cloned into pBluescript (Stratagene, La Jolla, CA) or pCRIITOPO plasmid vectors (Invitrogen, Carlsbad, CA) and sequenced using an automatic sequencer (ABI 3100, Applied Biosystems, Foster City, CA).

In situ hybridization

DNA templates were made by linearizing pBluescript or pCRIITOPO plasmids containing *Hox* inserts ranging from 300 to 800 bp. Antisense and sense RNA probes were generated by in vitro transcription using the DIG RNA Labeling Kit (Roche, Basel, Switzerland) according to the manufacturer's protocol. Whole-mount in situ hybridizations were performed as described by Murakami et al. (2001). For in situ hybridization, embryos were embedded in paraffin after fixation, sections (8 μm) were cut, and the deparaffinized sections were treated with 0.1 M triethanolamine/1.0%

HCl/0.2% acetic anhydride. After incubation in hybridization buffer for 2 hr at 65°C, slides were incubated at 65°C overnight in hybridization buffer containing DIG-labeled RNA probe (0.1 μg/μl). Sections were washed in 0.2 × SSC at 65°C and at room temperature for 30 min each, incubated in 1.5% blocking reagent (Roche) for 60 min, and then incubated with anti-digoxigenin–AP Fab fragment (Roche) diluted in 1.5% blocking reagent (1:4000) at room temperature for 2 hr. The antibody detection reaction was performed as previously described (Murakami et al., 2001).

Whole-mount immunostaining and morphological analyses

For morphological examinations and to determine the axial levels of the *Hox* expression boundaries in the embryos, we immunostained whole-mount embryos using 3A10 antibody directed against neurofilament (DSHB, Iowa City, IA) and MF20 antibody directed against myosin (DSHB), as previously described (Murakami et al., 2001). Briefly, primary antibodies were diluted 1:200 in aqueous 1% periodic acid and 5% nonfat dry milk in 10 mM Tris-HCl (pH 7.5) containing 0.5 M NaCl and 0.1% Tween 20 (TST). Samples were incubated at room temperature. Embryos were washed five times in TST for 1 hr each, followed by incubation overnight with horseradish peroxidase (HRP)-conjugated goat anti-rabbit IgG (Zymed, South San Francisco, CA) at a concentration of 1:1000 in aqueous 1% periodic acid and 5% nonfat dry milk in TST. The antibody was detected with 0.05 mg/ml diaminobenzidine and 0.02% H_2O_2 in TST at pH 5.5.

RESULTS

Comparison of axial specification in P. sinensis, chicken, and mouse

Using whole-mount turtle, chicken, and mouse embryos at mid-pharyngula stage immunostained with 3A10 and MF20 or stained with alcian blue, together with previous descriptions (Keibel and Mall,'10; de Beer,'37; Kuratani et al.,'88; Kessel,'92; Burke et al.,'95; Spörle and Schughart,'97), we compared the patterns of axial specification between *P. sinensis* and other amniote embryos (Figs. 1 and 2).

The thoracic vertebrae of *P. sinensis*, chicken, and mouse are defined as those associated with the long ribs (Ashley,'55; Romer,'56; Bellairs and Osmond,'98). Caudal to the occipital bones, there

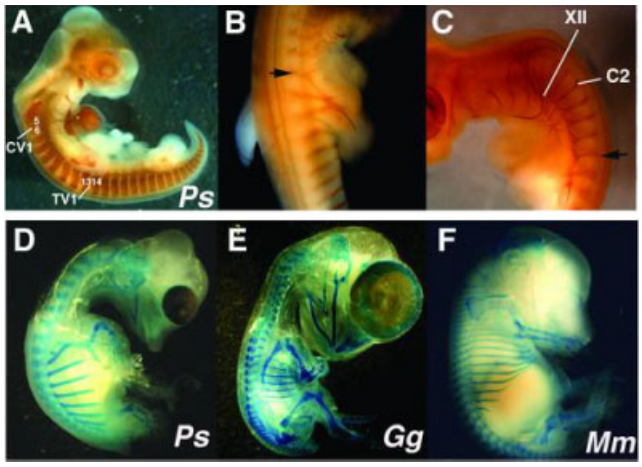

Fig. 1. Axial formulae of *P. sinensis*, chicken, and mouse embryos. (A) Stage 13–14 *P. sinensis* embryo stained with MF20 and 3A10. Somite numbers and the position of the first cervical (CV1) and the first thoracic (TV1) vertebrae are indicated. (B,C) Stage 13–14 *P. sinensis* embryo stained with 3A10. Black arrow indicates the most anterior spinal nerve contributing to the brachial plexus. The position of the hypoglossal nerve (XII) and the second cervical nerve are indicated. (D) Stage 18 *P. sinensis* embryo stained with alcian blue. (E) Stage 36 chicken embryo stained with alcian blue. (F) E14.5 mouse embryo stained with alcian blue.

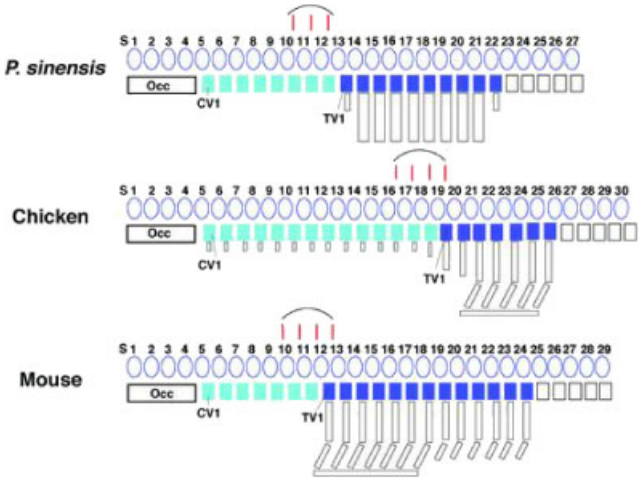

Fig. 2. Schematic representation of the axial formulae of *P. sinensis*, chicken, and mouse embryos. The somites are shown as ovals, the vertebrae as squares (white long squares represent the occipital vertebrae, green squares represent the cervical vertebrae, and blue squares represent the thoracic vertebrae). The vertical squares arising from the vertebrae represent the ribs. The spinal nerves contributing to the brachial plexus are represented by red bars. The level of the forelimb is indicated with a black curved line.

are eight cervical and 10 thoracic vertebrae in *P. sinensis* (Fig. 1D) (Ashley,'55), 14 cervical vertebrae and seven thoracic vertebrae in chicken (Fig. 1E) (Burke et al.,'95), and seven cervical

vertebrae followed by 13 thoracic vertebrae in mouse (Fig. 1F) (Burke et al.,'95).

In the chicken, the first four and a half somites (s) differentiate into occipital vertebrae, s5/6 into the atlas, and s6/7 into the axis (Couly et al.,'93). In mammals, including the mouse, and in *P. sinensis*, the somite number forming the occipital bone appears to be the same as in the chicken (de Beer,'37; Kessel,'92), consistent with the number of rootlets included in the hypoglossal nerve rostral to the atlas (see below).

In the chicken, the rostral spinal nerves (O1–C2) form the hypoglossal nerve (Kuratani et al.,'88), and the brachial plexus is made of CV12 to TV1, which arise at s16–20. The first thoracic vertebra (TV1) develops from s19/20 (Burke et al.,'95; Gaunt, 2000). Similarly, in *P. sinensis*, the rostral spinal nerves form the hypoglossal nerve and the brachial plexus consists of CV6 to CV8 (Fig. 1A–C). The numbering of the occipitospinal nerves is consistent with the number of occipital somites assumed by de Beer ('37), and with the anatomical description of the brachial plexus by Sieglbauer ('09). Thus, in *P. sinensis,* TV1 develops from s13/14 (Fig. 1A). In mouse, the brachial plexus is formed from CV5 to TV1, and TV1 develops from s12/13 (Burke et al.,'95; Gaunt, 2000).

By comparing the elements of this scheme (Fig. 2), it becomes clear that different numbers of segments and nerves differentiate into morphologically equivalent structures in each species. The following description is based on the axial specification levels shown in this scheme.

Cloning of P. sinensis, chicken, and mouse Hox genes

To isolate *P. sinensis Hox* cDNAs, we designed degenerate primers corresponding to the conserved regions in reported sequences of amniote *Hox* genes and isolated several different fragments of about 300–800 bp. The molecular phylogenetic analyses based on the neighbor-joining method (Saitou and Nei,'87) indicated that these cDNAs were *P. sinensis* orthologs of *Hoxa-5*, *Hoxb-5*, *Hoxc-6*, *Hoxa-7*, *Hoxb-7*, and *Hoxc-8* (Fig. 3). The partial sequences have been assigned DDBJ/EMBL/GenBank accession numbers AB193107–AB193111-115. We also isolated chicken cDNAs for *Hoxb-5* (accession number AB193110), *Hoxc-6* (accession number AB193109), *Hoxa-7*, *Hoxb-7* (accession number AB193108), and *Hoxc-8*, and mouse cDNA for *Hoxc-6*.

Comparative expression analysis of Hox genes

Using digoxigenin-labeled RNA probes synthesized from the isolated *Hox* cDNAs, we performed in situ hybridization on whole-mount and sectioned specimens of *P. sinensis*, chicken, and mouse embryos.

Hoxa-5 and Hoxb-5

By our whole-mount in situ hybridization, only a low level of expression could be detected for *Hoxa-5* (Fig. 4A). It was possible, however, to detect the specific distribution of transcripts in the myotome, which was restricted to the myotome at the cervical level (6th to 13th myotomes; Fig. 4B). Interestingly, the transcripts were absent from the myotomes at the thoracic levels (Fig. 4B). Expression was also seen in the neural tube from the transitional level between the hindbrain and the spinal cord to the level corresponding to s11/12 or the anlage of CV7 (data not shown). A similar expression pattern was observed in earlier-stage embryos (data not shown).

PsHoxb-5 expression in the stage 14 *P. sinensis* embryo was restricted to the cervical level of the neural tube, and weak expression was also detected in somites between the levels of s5/6 (CV1) and s11/12 (CV7) (Fig. 4C). No differences in their expression patterns were observed in an earlier-stage embryo (Fig. 4E). In a sectioned embryo, expression was detected only at the

Fig. 3. Molecular phylogenetic trees of *P. sinensis Hox* genes. The trees were inferred separately for paralogue groups (PG) 5 (A), -6 (B), -7 (C), and -8 (D), using the neighbor-joining method (Saitou and Nei,'87) with among-site rate heterogeneity taken into account (Yang,'94). The genes of *P. sinensis* are highlighted in black, and those of chicken in gray. The bootstrap values were calculated with 100 replicates. We used the amino acid sites that were unambiguously aligned with no gaps in the multiple alignments constructed by the alignment editor XCED, in which the MAFFT program is implemented (Katoh et al., 2002) and also by manual inspection. The numbers of amino acid sites used for each tree were as follows: (A) 83 amino acid sites; (B) 116 amino acid sites; (C) 97 amino acid sites; and (D) 162 amino acid sites. Accession numbers for the entries found in GenBank are indicated in parentheses. Otherwise, the accession numbers have been shown in the text. As outgroups, the genes belonging to the same PG but on different clusters were used. Analyses for PG5 (A) and PG7 (C) were presented as a composite tree, in which genes on one cluster serve as outgroups for the genes on the other (Gogarten et al.,'89; Iwabe et al.,'89). In the PG5 tree (A), the C cluster genes were excluded due to their high evolutionary rates.

cervical level (Fig. 4F). In a stage 24 chicken embryo, which roughly corresponds to stage 14 *P. sinensis*, uniform *Hoxb-5* expression was detected

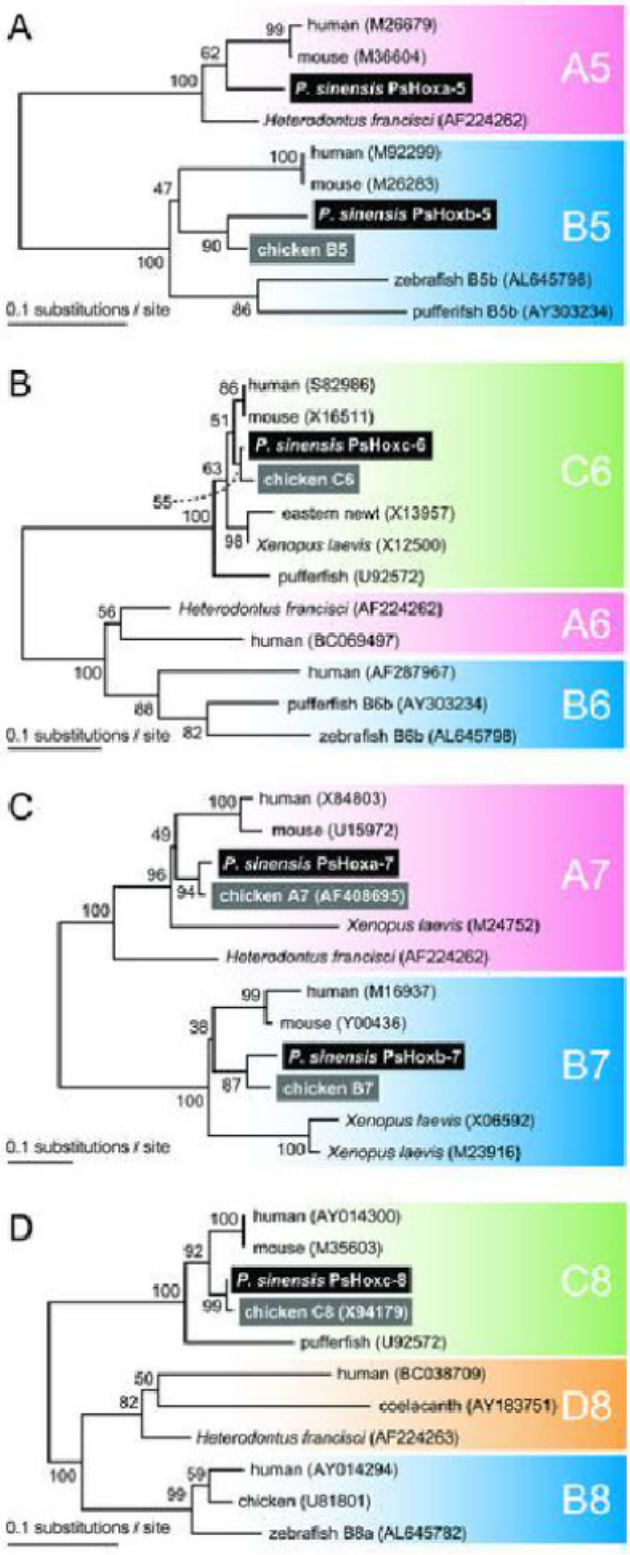

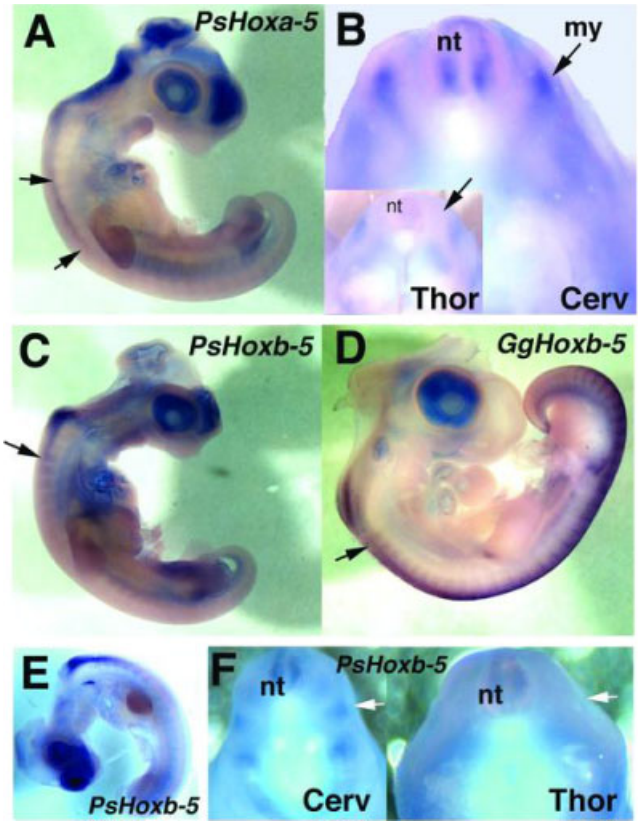

Fig. 4. *Hoxa-5* and *Hoxb-5* expression in *P. sinensis* and chicken embryos. (A) *PsHoxa-5* expression pattern in *P. sinensis* embryo (stage 14) using whole-mount in situ hybridization. Expression is detected in the neural tube and somites only at the cervical level. Black arrows indicate the anterior limit (s6/7, corresponding to the second cervical vertebra, CV2) and the posterior limit (s13/14; TV1) of gene expression in the somites at the cervical level. (B) Cross-section of embryo treated as in (A) at the cervical and thoracic levels. Black arrows indicate the dorsal region of myotomes both in the cervical and the thoracic sections. Clear signal is detected only in the cervical level myotome. The staining of the dorsolateral dermis at the thoracic level is background. (C, D) *Hoxb-5* expression pattern in *P. sinensis* (C, stage 14) and chicken (D, stage 24) using whole-mount in situ hybridization. (C) A weak signal is seen in the neural tube and somites. Expression is restricted within the cervical level. Black arrow indicates the anterior limit (s5/6 corresponding to CV1) of gene expression in the somites. (D) Expression is detected in the neural tube and somites from the cervical level to the caudal level. Black arrow indicates the anterior limit (s5/6; CV1) of gene expression in the paraxial mesoderm. (E) Ps*Hoxb-5* expression pattern in an earlier-stage *P. sinensis* embryo (stage 13). The pattern of expression is similar to (C). (F) Cross-section of embryo treated as in (E) at the cervical and thoracic levels. Signal is seen in the neural tube and somites only at the cervical level. White arrows indicate the region of somites both in the cervical and the thoracic sections. Signal is detected only in the somites of the cervical section. Abbreviations: my, myotome; nt, neural tube.

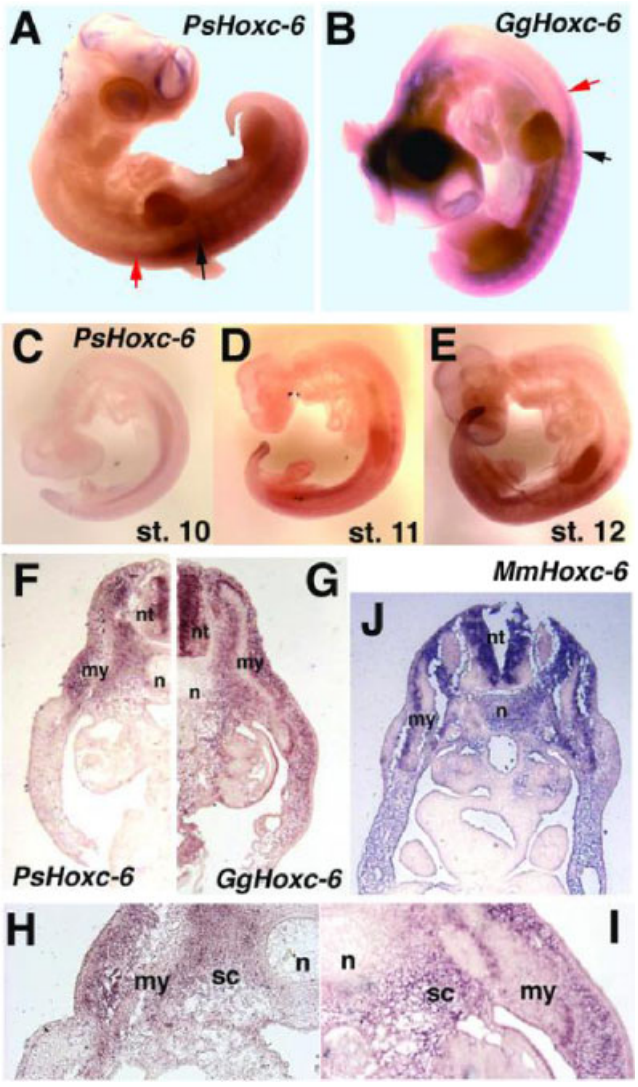

Fig. 5. *Hoxc-6* expression in *P. sinensis* and chicken embryos. (A, B) *Hoxc-6* expression patterns in *P. sinensis* (A; stage 13) and chicken (B; stage 24) using whole-mount in situ hybridization. (A) The black arrow indicates the anterior limit (s13/14; TV1) of gene expression in the somites, and the red arrow indicates the anterior limit in the CNS. (B) The black arrow indicates the anterior limit (s19/20; TV1) of gene expression in the somites, and the red arrow indicates the anterior limit in the CNS. (C–E) *PsHoxc-6* expression pattern in developing *P. sinensis* embryo (stages 10–12) using whole-mount in situ hybridization. *PsHoxc-6* expression begins before stage 10 and the signal at the thoracic level becomes stronger as development proceeds. (F) Histological analysis of *Hoxc-6* expression in *P. sinensis* (F; stage 13) and chicken (G; stage 24) embryos at the thoracic level. (H, I) High magnification of (F) and (G), respectively. In the chicken, expression was detected in the neural tube, the neural arch, the prevertebrae, the lips of myotomes, the dorsal dermis, and the somatopleure (G, I), whereas in *P. sinensis*, no expression was detected in the somatopleure (F, H). (J) Histological analysis of *Hoxc-6* expression in the mouse (E10.5) at the thoracic level. Expression was detected in the neural tube, the neural arch, the prevertebrae, the dorsal dermis, and the somatopleure. Abbreviations: my, myotome; n, notochord; nt, neural tube; sc, sclerotome.

in the central nervous system (CNS) from the transitional area between the hindbrain and the spinal cord to the level of the posteriormost somite (Fig. 4D). Expression was also seen in the somites from the level of s5/6 (CV1) to the last somite.

Hoxc-6

Hoxc-6 cognates displayed anterior expression boundaries in somites at the level of the first thoracic vertebra (TV1), in both *P. sinensis* and chicken embryos (Fig. 5A,B). In the stage 24 chicken embryo, a *Hoxc-6* signal was detected from the level of s19/20 (TV1) (Fig. 5B), and in the stage 13+ *P. sinensis* embryo, *PsHoxc-6* expression was seen from the level of s13/14 (TV1) (Fig. 5A). *PsHoxc-6* expression was initiated in the

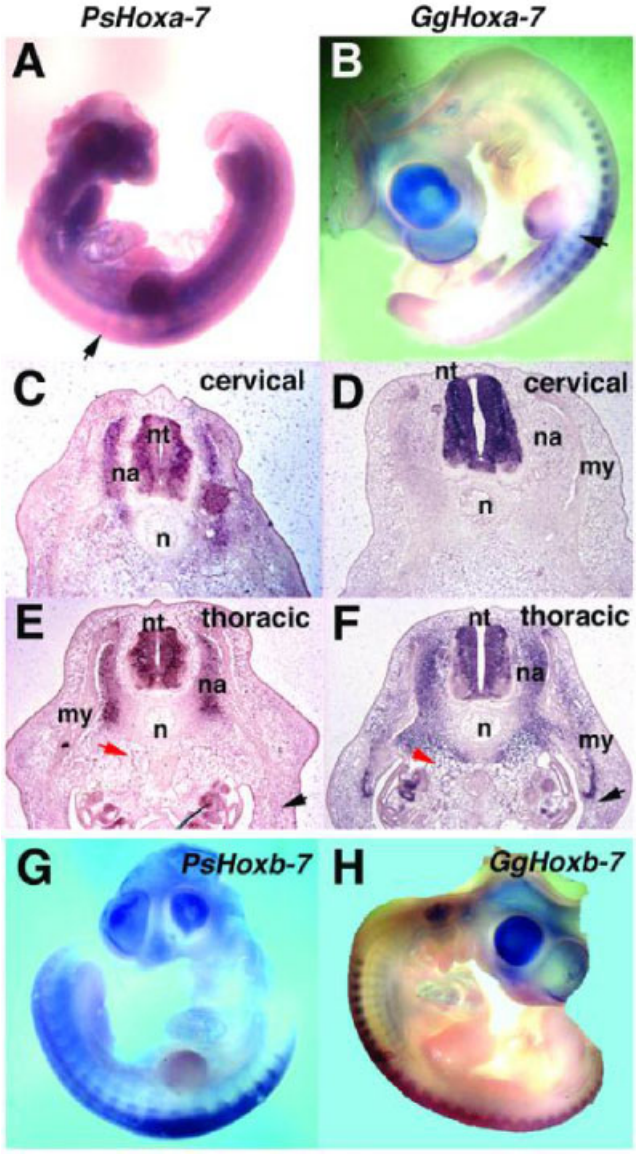

P. sinensis embryo before stage 10, and the signal became stronger as development proceeded (Fig. 5C–E). Histological analysis at the thoracic level of stage 13+ *P. sinensis* embryos (roughly corresponding to HH stage 25 in the chicken) showed that the expression of *PsHoxc-6* was restricted to the sclerotome (prevertebra) and the dermis in the epaxial domain (future carapacial dermis). This differs from the chicken, where *Hoxc-6* expression was also detected in the somatopleure (compare Fig. 5G and I with Fig. 5F and H). In the E10.5 mouse embryo, *Hoxc-6* was expressed in the somatopleure at the thoracic level, in a pattern similar to that in the chicken (Fig. 5J). In both *P. sinensis* and chicken, strong expression of *Hoxc-6* was seen in the spinal motor neurons (MN) at the forelimb level (Fig. 5A,B). In the chicken, the posterior boundary of *Hoxc-6* expression in the CNS was observed at the level of s20/21 (TV2), and in *P. sinensis*, the posterior boundary was at the level of s13/14 (TV1), thus corresponding to the level of the forelimb in each animal.

Hoxa-7 and Hoxb-7

In the stage 14 *P. sinensis* embryo, the anterior boundary of *PsHoxa-7* expression in the somites was observed at the level of s10/11 (CV6) (Fig. 6A). Histological analysis showed that *PsHoxa-7* transcripts at this level were localized in the neural arch, as well as in the neural tube and the dorsal root ganglia (DRG) (Fig. 6C). At the thoracic level, the expression of *PsHoxa-7* was seen in the neural arch and the neural tube (Fig. 6E). In the stage 24 chicken embryo, the anterior boundary of *Hoxa-7* expression in the CNS was detected at the level of s10/11 (CV6) (Fig. 6B). Histological analysis showed signals in the neural tube and the DRG (Fig. 6D). The anterior boundary of somitic expression was observed at the level of s20/21 (TV2) (Fig. 6B), and transcripts were detected in the neural arch, dorsal dermis, prevertebrae, and the lips of myotomes (Fig. 6F). In *P. sinensis* embryos, no signals were detected in the myotomes (Fig. 6E). In contrast, in chicken embryos, transcripts of *Hoxa-7* were not seen in the cervical neural arch (Fig. 6D).

Expression of *Hoxb-7* cognates was detected in the neural tube and the DRG along the entire neuraxis in *P. sinensis* and chicken embryos (Fig. 6G,H). However, no expression of *Hoxb-7* was detected in somites, in either *P. sinensis* or chicken embryos.

Fig. 6. *Hoxa-7* and *Hoxb-7* expression in *P. sinensis* and chicken embryos. (A, B) *Hoxa-7* expression patterns in *P. sinensis* (A; stage 13+) and chicken (B; stage 24) embryos using whole-mount in situ hybridization. (A, B) The black arrows indicate the anterior limits of gene expression (s10/11, CV6 in *P. sinensis*; s20/21, TV2 in chicken) in the somites. (C–F) Histological analysis of *Hoxa-7* expression in *P. sinensis* (C, E) and chicken (D, F) embryos at the cervical and thoracic levels. At the cervical level, expression was detected in the neural tube and neural arch in *P. sinensis* (A, C) and only in the neural tube in the chicken (B, D), as well as in the DRG (data not shown). At the thoracic level, expression of *Hoxa-7* was detected in the neural tube and the neural arch in *P. sinensis* (E), whereas in chicken, expression was detected in the neural tube, the neural arch, the prevertebrae, and the tips of myotomes (F). (E, F) The red arrows indicate the site of the prevertebrae, and the black arrows indicate the tips of myotome. (G, H) *Hoxb-7* expression patterns in *P. sinensis* (G; stage 13) and chicken (H; stage 24) embryos using whole-mount in situ hybridization. Expression of *Hoxb-7* cognates was detected in the neural tube and the DRG along almost the entire length of the body in both *P. sinensis* and chicken embryos. Abbreviations: my, myotome; n, notochord; neural arch; nt, neural tube.

Hoxc-8

The expression patterns of *Hoxc-8* cognates were very similar in the chicken and *P. sinensis* (Fig. 7A,B): the anterior limits of expression were found at the level of s15/16 (TV3) in the stage 14 *P. sinensis* embryo (Fig. 7A), and of s23/24 (TV5) in the stage 24 chicken embryo (Fig. 7B). Histological analyses showed that *Hoxc-8* was expressed in the dorsal dermis, the prevertebrae, and the somatopleure at the thoracic level in both animals (Fig. 7C,D).

DISCUSSION

As has been suggested several times, changes in the developmental patterning of the mesoderm appear to have resulted in carapace formation in the turtle (Hall,'98). Those changes are restricted to the mesodermal derivatives at certain levels of the axial structure, implying that they were introduced into the developmental cascade acting downstream from the *Hox* code (Nowicki and Burke, 2003b), and/or the *Hox* code itself underwent turtle-specific changes at the appropriate specific axial level. We detected no deficiency, disruption, or duplication in the *P. sinensis Hox* genes, although our dataset is a limited one. Therefore, no *P. sinensis*-specific genes seem to act uniquely in carapacial patterning. Moreover, the homeodomains of the isolated genes are perfectly conserved between the *Hox* genes of *P. sinensis* and those of the other amniotes (data not shown), implying that the DNA-binding

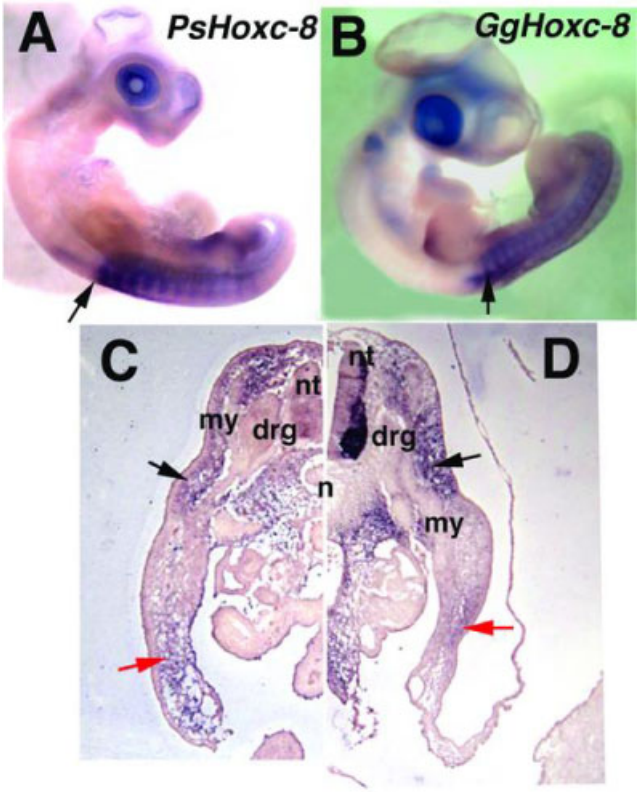

Fig. 7. *Hoxc-8* expression in *P. sinensis* and chicken embryos. (A, B) *Hoxc-8* expression patterns in *P. sinensis* (A; stage 13+) and chicken (B; stage 24) embryos using whole-mount in situ hybridization. In both animals, transcripts were detected in the somites at the thoracic level. Black arrows indicate the anterior limits of gene expression in the somites (s15/16, TV3 in *P. sinensis*; s23/24, TV5 in chicken). (C, D) Histological analysis of *Hoxc-8* expression in *P. sinensis* (C; stage 13+) and chicken (D; stage 24) embryos at the thoracic level. (C, D) The black arrows indicate expression in the dorsal dermis, and the red arrows indicate expression in the somatopleure. Abbreviations: my, myotome; n, notochord; nt, neural tube; drg, dorsal root ganglia.

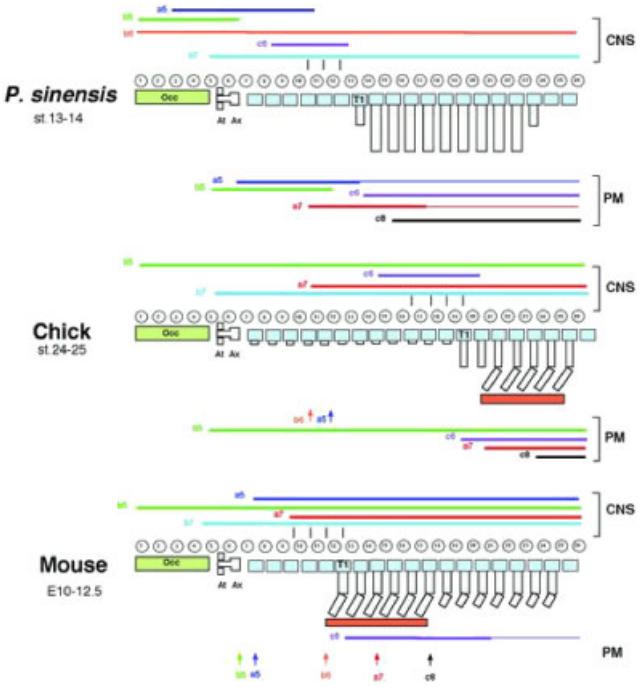

Fig. 8. Schematic representation of *Hox* gene expression in *P. sinensis*, chicken, and mouse embryos. Horizontal lines show the regions of expression of the *Hox* genes in the CNS or the somites. Arrows show the anterior boundaries of *Hox* gene expression. The somites are shown as ovals, the vertebrae as light blue squares. Large anterior squares represent the fused occipital vertebrae. The vertical squares arising from the vertebrae represent the ribs. Orange squares represent the sternum. The spinal nerves contributing to the brachial plexus are represented by vertical lines. The data for the mouse are derived from Burke et al. ('95), Rancourt et al. ('95), Gaunt et al. ('99), and Gaunt (2000).

specificity of the *P. sinensis Hox* gene products per se have not changed during turtle evolution. The distribution of transcripts, however, may have undergone turtle-specific changes in accordance with the changes in body plan. As the first step in explaining the molecular events involved in this evolutionary innovation, we attempted comparative analyses of amniote morphology by examining the expression patterns of *Hox* genes in *P. sinensis*, chicken, and mouse embryos.

In a comparison of *Hox* expression patterns in the cervical and thoracic regions of the three amniote species (Fig. 8), we found possibly turtle-specific patterns, some of which may be associated with this unique body plan. Exceptionally, the expression pattern of *Hoxb-7* is shared by *P. sinensis* and chicken, implying that the regulation of this gene was established in their common ancestor and/or it was irrelevant to the establishment of turtle-specific developmental plan. Also, the unique expression pattern of *Hoxa-7* in *P. sinensis* does not seem to be associated with any overt body plan element of this animal. Therefore, it is possible that some of the changes in the *Hox* gene expression domains are neutral, both in terms of evolutionary changes and in their developmental function. In the following discussion, we will focus on *P. sinensis*-specific traits in *Hox* expression that are coincidental with the turtle-specific patterning program.

Changes in the expression patterns of PsHoxc-6 and PsHoxc-8 may reflect the turtle-specific body plan

Burke et al. ('95) have demonstrated that the anterior boundary of *Hoxc-6* expression in the

somites corresponds to the position of the last spinal nerve of the brachial plexus in various vertebrates. In amniotes, therefore, this expression border is located at the somites that map to TV1, implying that *Hoxc-6* determines thoracic identity. Consistent with this, over-expression of *Hoxc-6* in the mouse lumbar vertebrae results in the formation of ectopic ribs (Jegalian and De Robertis,'92). The expression pattern of *PsHoxc-6* also seems consistent with this A–P specification in amniotes. In histological studies, however, a clear difference was observed between the turtle and other amniotes. In chicken and mouse, *Hoxc-6* signals were distributed in both the dorsal dermis and the somatopleure, whereas no signal was detected in the somatopleure of *P. sinensis*. Because *Hoxc-6* expression in the somatopleure is conserved between mammals and birds, this may represent the primitive expression pattern for amniotes (see below). The absence of *PsHoxc-6* expression in the somatopleure of *P. sinensis* thus appears to be unique to this animal, and may be coincidental with the turtle-specific body plan. As already noted, the most conspicuous difference between turtles and other amniotes at the thoracic level is the position and structure of the ribs, which are somite derivatives (Christ et al.,'74; Huang et al.,'94,'96, 2000; Kato and Aoyama,'98; Nowicki and Burke, 2003a). In other amniotes, the body of the rib is composed of the dorsal (vertebral) rib and the (ventral) sternal rib, whereas in turtles, the vertebral ribs only grow laterally to form the dorsal carapace (Ruckes,'29). There is as yet no report of the formation of the ventral rib during development in turtles. The loss of expression of *Hoxc-6* in the *P. sinensis* somatopleure coincides with the embryonic region in which the ventral ribs are specifically missing in turtles.

In this context, Nowicki and Burke (2003b) recently found that, in the chicken, somite-derived mesenchyme migrates as a primaxial element into the somatopleure (adaxial domain) to form the ribs and surrounding tissues. It would be of particular importance to determine if the *Hoxc-6* expression is restricted to somite-derived cell lineages in *P. sinensis* and to compare the migration patterns of somite-derived cells between chicken and *P. sinensis*. Also intriguing would be loss-of-function experiments for *Hoxc-6* in the mouse or chicken somatopleure and gain-of-function experiments in the turtle somatopleure, which may give us some information about ventral rib formation in the amniotes and the disappearance of the ventral ribs in turtles.

Also coincident with turtle-specific patterning is the expression of *Hoxc-8*, *Hoxa-5*, and *Hoxb-5*. The anterior border of *Hoxc-8* expression is in the somites at the midthoracic level in both chicken and mouse (Burke et al.,'95). In the ventral part of the body, the level of *Hoxc-8* expression is associated with the absence among amniotes of ribs articulating to the sternum (coincidental with the lumbar region in mammals; Fig. 8). Consistent with this, the addition of sternebrae and an increase in the number of ribs that touch the sternum were observed in *Hoxc-8*-mutant mice (Le Mouellic et al.,'92). In *P. sinensis*, the anterior border of *PsHoxc-8* expression is unusually anterior (TV3), consistent with the loss of the sternum and ventral ribs in the turtles. Similarly, the expression levels of *Hoxa-5* and *Hoxb-5* correspond to the origin of the scapula; disruption of *Hoxa-5* in mice leads to anomalies in the acromion (Aubin et al., 2002), and disruption of *Hoxb-5* results in a rostral shift in the shoulder girdle (Rancourt et al.,'95). These genes are expressed at similar axial levels in the chicken and mouse (Gaunt, 2000; Aubin et al., 2002). Experimental studies have also suggested that the turtle scapula originates from s8–12 (CV4–7), and that of the chicken from s15–24 (CV11–TV5) (Burke,'91). The expression of *Hoxa-5* and *Hoxb-5* in *P. sinensis* is restricted to the cervical region and apparently coincides with the hypothetical transposition of somite identities to form the shoulder girdle.

Acquisition of the turtle-specific body plan and evolution of the Hox code

The evolution of the body plan can be viewed as a series of changes in the developmental patterning programs of organisms. Without doubt, phylogenetic changes in the *Hox* code are a central element in our understanding of axial skeletal evolution, including the invention of the turtle carapace. As described above, *Hox* gene expression in *P. sinensis* differs from that in chicken and mouse in a number of respects. These differences may underlie the turtle-specific body plan, although comparisons with other turtles are necessary to confirm that these expression patterns are widespread among turtle species. This raises further questions: Were all the turtle-specific features of *Hox* gene expression newly acquired in the turtle lineage? If so, when and how were they acquired in phylogenetic history? These questions are inherently associated with the

phylogenetic position of turtles with respect to the other amniotes, which has itself been a matter of debate for more than a century.

There are two basic classes of hypothetical scenario used to explain the phylogenetic position of the turtles. One of these assumes that turtles are primitive amniotes, or anapsids, a sister group of all other extant amniotes (Gaffney,'80; Colbert et al., 2001). The other class, on the other hand, proposes that mammals (or synapsids, including mammals) are the most basal living amniotes and places the turtles after the divergence of mammals, crownward on the phylogenetic tree (Rieppel and deBraga,'96; Lee,'97; Platz and Conlon,'97; Reisz,'97; Zardoya and Meyer,'98; Hedges and Poling,'99; Kumazawa and Nishida,'99; Mannen and Li,'99; Cao et al., 2000; Zardoya and Meyer, 2001). In this second class of theories, some authors regard turtles as archosaurians (Platz and Conlon,'97; Zardoya and Meyer,'98; Hedges and Poling,'99; Kumazawa and Nishida,'99; Mannen and Li,'99; Cao et al., 2000; Zardoya and Meyer, 2001). However, neither of these hypotheses has become predominant, and it is agreed that each is based on evidence that is to some extent questionable (Gauthier et al.,'88).

The present study is intended neither to postulate the ancestral *Hox* code of the amniotes nor to clarify the phylogenetic position of the turtles. Nevertheless, comparison of *Hoxc-6* expression levels in *Xenopus*, zebrafish, and amniote species seems to indicate that the primitive amniote *Hox* code was established with a posterior shift in the *Hoxc-6* expression domain, together with the establishment of the neck region that is unique to amniotes (Burke et al.,'95). Undoubtedly, the turtle *Hox* code must have been acquired by modification of one such amniote prototype.

Irrespective of the uncertainty regarding its phylogeny, it is possible that many of the turtle-specific features described herein might actually represent a developmental synapomorphy. If the turtles are archosaurians and closely related to the avians, the features of the gene expression patterns shared by chicken and mouse probably represent primitive features of the amniote *Hox* code, whereas the turtle-specific features may have been acquired secondarily in the turtle lineage. On the contrary, if turtles represent a basal group of amniotes, they clearly show a different body plan from those of fossil stem reptiles. If this is the case, the turtle may possess a number of turtle-specific features in their developmental program, including modifications to the *Hox* code. In either case, it is possible that some of the *P. sinensis*-specific features of *Hox* expression identified in this study are actually related to the turtle-specific trunk developmental program. The similarity in the amino acid sequences of the *Hox* genes between chicken and *P. sinensis* also permits us to speculate that changes in their regulation, not in the Hox proteins themselves, were responsible for the evolution of the turtle-specific body plan. To test this hypothesis, further manipulations involving gain- and loss-of-function experiments are required, which are within the scope of our future projects.

More examples must be studied from more animal groups before we attempt to draw any conclusive scenarios for the *Hox* code and the axial skeletal evolution. We should bear in mind that neither the mouse nor the chicken is necessarily a basal representative of mammals or birds. When a robust phylogeny becomes available in the future, we will be able to distinguish primitive and secondary features in the *Hox* codes of various animals and to ask which changes in the regulatory mechanisms of these genes were responsible for the establishment of specific body plans.

ACKNOWLEDGMENTS

We thank Hiroshi Nagashima and Masumi Nakazawa for their technical assistance and Takuya Murata and Shinichi Aizawa for the mouse cDNA library. We also thank Ann C. Burke for her critical reading of the manuscript. The monoclonal antibodies (MF20, developed by Donald A. Fischman, and 3A10, developed by Thomas M. Jessell and Jane Dodd) were obtained from the Developmental Studies Hybridoma Bank, where they were developed under the auspices of the NICHD and maintained by the University of Iowa, Department of Biological Sciences (Iowa City, IA). This work was supported by Grants-in-Aid from the Ministry of Education, Science and Culture of Japan (Specially Promoted Research) to S.K.

LITERATURE CITED

Ashley LM. 1955. Laboratory Anatomy of the Turtle. Boston: WCB/McGraw-Hill.

Aubin J, Lemieux M, Moreau J, Lapointe J, Jeannotte L. 2002. Cooperation of *Hoxa5* and *Pax1* genes during formation of the pectoral girdle. Dev Biol 244:96–113.

Bellairs R, Osmond M. 1998. The atlas of chick development. San Diego: Academic Press.

Burke AC. 1989. Development of the turtle carapace: implications for the evolution of a novel bauplan. J Morphol 199:363–378.

Burke AC. 1991. The development and evolution of the turtle body plan. Inferring intrinsic aspects of the evolutionary process from experimental embryology. Am Zool 31:616–627.

Burke AC, Nelson CE, Morgan BA, Tabin C. 1995. *Hox* genes and the evolution of vertebrate axial morphology. Development 121:333–346.

Cao Y, Sorenson MD, Kumazawa Y, Mindell DP, Hasegawa M. 2000. Phylogenetic position of turtles among amniotes: evidence from mitochondrial and nuclear genes. Gene 259:139–148.

Chen F, Greer J, Capecchi MR. 1998. Analysis of *Hoxa7/b7* mutants suggests periodicity in the generation of the different sets of vertebrae. Mech Dev 77:49– 57.

Christ B, Jacob HJ, Jacob M. 1974. Experimental studies on the development of the thoracic wall in chick embryos. Experientia 30:1449–1451.

Colbert EH, Morales M, Minkoff EC. 2001. Colbert's evolution of the vertebrates, 5th edition. New York: Wiley & Sons Inc.

Condie BG, Capecchi MR. 1994. Mice with targeted disruptions in the paralogous genes *hoxa-3* and *hoxd-3* reveal synergistic interactions. Nature 370, 304–307.

Couly GF, Coltey P, Le Douarin NM. 1993. The triple origin of skull in higher vertebrates: a study in quail-chick chimeras. Development 117:409–429.

Davis AP, Witte DP, Hsiehli HM, Potter SS, Capecchi MR. 1995. Absence of radius and ulna in mice lacking *hoxa-11* and *hoxd-11*. Nature 375:791–795.

de Beer GR. 1937. The development of the vertebrate skull. London: Oxford University Press.

Favier B, Rijli FM, Fromental-Ramain C, Fraulob V, Chambon P, Dolle P. 1996. Functional cooperation between the non-paralogous genes *Hoxa-10* and *Hoxd-11* in the developing forelimb and axial skeleton. Development 122:449–460.

Fromental-Ramain C, Warot X, Lakkaraju S, Favier B, Haack H, Birling C, Dierich A, Dolle P, Chambon P. 1996. Specific and redundant functions of the paralogous *Hoxa-9* and *Hoxd-9* genes in forelimb and axial skeleton patterning. Development 122:461–472.

Gaffney ES. 1980. Phylogenetic relationships of the major groups of amniotes. In: Panchen AL, editor. The terrestrial environment and the origin of land vertebrates. San Diego: Academic Press. p 593–610.

Gaffney, ES. 1990. The comparative osteology of the Triassic turtle *Proganochelys*. Bull Am Mus Nat Hist 194:1–263.

Gaunt SJ. 2000. Evolutionary shifts of vertebrate structures and *Hox* expression up and down the axial series of segments: a consideration of possible mechanisms. Int J Dev Biol 44:109–117.

Gaunt SJ, Dean W, Sang H, Burton RD. 1999. Evidence that Hoxa expression domains are evolutionarily transposed in spinal ganglia, and are established by forward spreading in paraxial mesoderm. Mech Dev 82:109–118.

Gauthier J, Kluge AG, Rowe T. 1988. Amniote phylogeny and the importance of fossils. Cladistics 4:105–209.

Gavalas A, Studer M, Lumsden A, Rijli FM, Krumlauf R, Chambon P. 1998. *Hoxa1* and *hoxb1* synergize in patterning the hindbrain, cranial nerves and second pharyngeal arch. Development 125:1123–1136.

Gilbert SF, Loredo GA, Brukman A, Burke AC. 2001. Morphogenesis of the turtle shell: the development of a novel structure in tetrapod evolution. Evol Dev 3(2):47–58.

Goddard JM, Rossel M, Manley NR, Capecchi MR. 1996. Mice with targeted disruption of *Hoxb-1* fail to form the motor nucleus of the VIIth nerve. Development 122:3217–3228.

Gogarten JP, Kibak H, Dittrich P, Taiz L, Bowman EJ, Bowman BJ, Manolson MF, Poole RJ, Date T, Oshima T. 1989. Evolution of the vacuolar H^+-ATPase: implications for the origin of eukaryotes. Proc Natl Acad Sci U S A 86(17):6661–6665.

Hall BK. 1998. Evolutionary developmental biology, 2nd edition. London: Chapman & Hall.

Hamburger V, Hamilton HL. 1951. A series of normal stages in the development of the chick embryo. J Morphol 88:49–91.

Hedges SB, Poling LL. 1999. A molecular phylogeny of reptiles. Science 283:998–1001.

Horan GSB, Remirez-Solis R, Featherstone MS, Wolgemuth DJ, Bradley A, Behringer RR. 1995. Compound mutants for the paralogous *hoxa-4*, *hoxb-4*, and *hoxd-4* genes show more complete homeotic transformations and a dose-dependent increase in the number of vertebrae transformed. Genes Dev 9:1667–1677.

Huang R, Zhi Q, Wilting J, Christ B. 1994. The fate of somitocoele cells in avian embryos. Anat Embryol 190: 243–250.

Huang R, Zhi Q, Neubuser A, Muller TS, Brand-Saberi B, Christ B, Wilting J. 1996. Function of somite and somitocoele cells in the formation of the vertebral motion segment in avian embryos. Acta Anatomica 155:231–241.

Huang R, Zhi Q, Schmidt C, Wilting J, Brand-Saberi B, Christ B. 2000. Sclerotomal origin of the ribs. Development 127:527–532.

Iwabe N, Kuma K, Hasegawa M, Osawa S, Miyata T. 1989. Evolutionary relationship of archaebacteria, eubacteria, and eukaryotes inferred from phylogenetic trees of duplicated genes. Proc Natl Acad Sci U S A 86(23):9355–9359.

Jaekel O. 1916. Die Wirbeltierfunde aus dem Keuper von Halberstadt. Serie 11. Testudinata. Part 1. Paläont Z 2:88–214.

Jegalian BG, De Robertis EM. 1992. Homeotic transformations in the mouse induced by overexpression of a human *Hox3.3* transgene. Cell 71:901–910.

Kato N, Aoyama H. 1998. Dermomyotomal origin of the ribs as revealed by extirpation and transplantation experiments in chick and quail embryos. Development 125:3437–3443.

Katoh K, Misawa K, Kuma K, Miyata T. 2002. MAFFT: a novel method for rapid multiple sequence alignment based on fast Fourier transform. Nucleic Acids Res 30(14):3059–3066.

Keibel F, Mall FP. 1910. Manual of human embryology. Philadelphia: Lippincott.

Kessel M. 1992. Respecification of vertebral identities by retinoic acid. Development 115:487–501.

Krumlauf R. 1994. *Hox* genes in vertebrate development. Cell 78:191–201.

Kumazawa Y, Nishida M. 1999. Complete mitochondrial DNA sequences of the green turtle and blue-tailed mole skink: statistical evidence for archosaurian affinity of turtles. Mol Biol Evol 16:784–792.

Kuratani S, Tanaka S, Ishikawa Y, Zukeran C. 1988. Early development of the hypoglossal nerve in the chick embryo as observed by the whole-mount nerve staining method. Am J Anat 182:155–168.

Lee MSY. 1993. The origin of the turtle body plan: bridging a famous morphological gap. Science 261:1716–1720.

Lee MSY. 1997. Reptile relationships turn turtle… Nature 389:245–246.

Le Mouellic H, Lallemand Y, Brulet P, 1992. Homeosis in the mouse induced by a null mutation in the *Hox-3.1* gene. Cell 69:251–264.

Mak TW. 1998. The gene knockout facts book. San Diego: Academic Press.

Manley NR, Capecchi MR. 1997. *Hox* group 3 paralogous genes act synergistically in the formation of somitic and neural crest-derived structures. Dev Biol 192:274–288.

Mannen H, Li SL. 1999. Molecular evidence for a clade of turtles. Mol Phylogenet Evol 13:144–148.

Murakami Y, Ogasawara M, Sugahara F, Hirano S, Satoh N, Kuratani S. 2001. Identification and expression of the lamprey *pax6* gene: evolutionary origin of the segmented brain of vertebrates. Development 128:3521–3531.

Müller GF, Wagner GP. 1991. Novelty in evolution: restructuring the concept. Annu Rev Ecol Syst 22:229–256.

Nowicki JL, Burke AC. 2000. *Hox* genes and morphological identity: axial versus lateral patterning in the vertebrate mesoderm. Development 127:4265–4275.

Nowicki JL, Burke AC. 2003a. The lateral somitic frontier: dorso-ventral aspects of anterior–posterior regionalization in avian embryos. Mech Dev 120:227–240.

Nowicki JL, Burke AC. 2003b. A new view of patterning domains in the vertebrate mesoderm. Dev Cell 4:159–165.

Platz JE, Conlon JM. 1997. Reptile relationships turn turtle ... and turn back again. Nature 389:246.

Rancourt DE, Tsuzaki T, Capecchi MR. 1995. Genetic interaction between *hoxb-5* and *hoxb-6* is revealed by nonallelic noncomplementation. Genes Dev 9:108–122.

Reisz RR. 1997. The origin and early evolutionary history of amniotes. Trends Ecol Evol 12:218–222.

Rieppel O, deBraga M. 1996. Turtles as diapsid reptiles. Nature 384:453–455.

Rieppel O. 2001. Turtles as hopeful monsters. BioEssays 23:987–991.

Romer AS. 1956. The osteology of the Reptiles. Chicago: University of Chicago Press.

Ruckes H. 1929. Studies in chelonian osteology. Part II. The morphological relationships between the girdles, ribs and carapace. Ann N Y Acad Sci 31:81– 120.

Saitou N, Nei M. 1987. The neighbor-joining method: a new method for reconstructing phylogenetic trees. Mol Biol Evol 4(4):406–425.

Sieglbauer F. 1909. Zur Anatomie der Schildkrotenextremitat. Archiv Anat Phys Anat Abt 183–280.

Slack JMW, Holland PWH, Graham CF. 1993. The zootype and the phylotypic stage. Nature 361:490–492.

Spörle R, Schughart K. 1997. System to identify individual somites and their derivatives in the developing mouse embryo. Dev Dyn 210:216–226.

Studer M, Gavalas A, Marshall H, Ariza-McNaughton L, Rijli FM, Chambon P, Krumlauf R. 1998. Genetic interactions between *hoxa1* and *hoxb1* reveal new roles in regulation of early hindbrain patterning. Development 125: 1025–1036.

Suemori H, Noguchi S. 2000. *Hox C* cluster genes are dispensable for overall body plan of mouse embryonic development. Dev Biol 220: 333–342.

Theiler K. 1989. The house mouse. Atlas of embryonic development. New York: Springer- Verlag.

Tiret L, Le Mouellic H, Maury M, Brulet P. 1998. Increased apoptosis of motoneurons and altered somatotopic maps in the brachial spinal cord of *Hoxc-8*-deficient mice. Development 125:279–291.

Tokita M, Kuratani S. 2001. Normal embryonic stages of the Chinese soft-shelled turtle *Pelodiscus sinensis* (Tryonychidae). Zool Sci 18:705–715.

Vieille-Grosjean I, Hunt P, Gulisano M, Boncinelli E, Thorogood P. 1997. Brachial *HOX* gene expression and human craniofacial development. Dev Biol 183:49–60.

Yang Z. 1994. Maximum likelihood phylogenetic estimation from DNA sequences with variable rates over sites: approximate methods. J Mol Evol 39:306–314.

Zardoya R, Meyer A. 1998. Complete mitochondrial genome suggests diapsid affinities of turtles. Proc Natl Acad Sci USA 95:14226–14231.

Zardoya R, Meyer A. 2001. The evolutionary position of turtles revised. Naturwissenschaften 88:193–200.